InAsSb/InP quantum dots for midwave infrared emitters: A theoretical study

ARTICLE *in* JOURNAL OF APPLIED PHYSICS · DECEMBER 2005

Impact Factor: 2.18 · DOI: 10.1063/1.2143115

7 AUTHORS, INCLUDING:

Ana Ballestar
Graphene Nanotech, S. L.
29 PUBLICATIONS **129** CITATIONS
SEE PROFILE

J. Even
Institut National des Sciences Appliquées de …
334 PUBLICATIONS **1,615** CITATIONS
SEE PROFILE

N. Bertru
Institut National des Sciences Appliquées de …
182 PUBLICATIONS **1,274** CITATIONS
SEE PROFILE

Alain le corre
Institut National des Sciences Appliquées de …
338 PUBLICATIONS **2,210** CITATIONS
SEE PROFILE

InAsSb/InP quantum dots for midwave infrared emitters: A theoretical study

C. Cornet,[a] F. Doré, A. Ballestar, J. Even, N. Bertru, A. Le Corre, and S. Loualiche
LENS-UMR FOTON 6082 au CNRS INSA de Rennes, 20 Avenue des Buttes de Coesmes, CS 14315, F34043 Rennes Cedex, France

(Received 10 May 2005; accepted 3 November 2005; published online 29 December 2005)

A theoretical study of the electronic properties of InAsSb quantum dots (QDs) deposited on InP substrate is presented. Unstrained bulk materials present a direct gap between 0.1 and 0.35 eV suitable for mid-infrared emitters (2–5 μm). However, strain and quantum-confinement effects may limit the extension of the emission spectrum of these nanostructures towards the higher wavelengths. Various associations of materials in the barrier are considered. Among the possible associations, $InAs_{0.5}Sb_{0.5}/GaAs_{0.5}Sb_{0.5}$ QDs may provide a low-energy emission with a material system similar to the well-known InAs/GaAs system. Other materials associations such as InAsSb/InGaAsP/InP are also studied. Band lineups, optical transitions, optical losses, and effective masses are computed and discussed. © *2005 American Institute of Physics*.
[DOI: 10.1063/1.2143115]

Efficient semiconductor lasers emitting in the near-infrared range (2–5 μm) at room temperature (RT) have great potential in applications such as laser radar, military countermeasure, pollution monitoring, and molecular spectroscopy. Laser diodes based on a GaInAsSb/AlGaAsSb type I quantum well (QW) have exhibited excellent RT characteristics up to 2.7 μm.[1,2] However, these type I laser diodes cannot reach higher wavelength because of the band lineups between arsenide and antimony. At long wavelengths (8–12 μm range), quantum cascade (QC) lasers based on the transition between confined states within the conduction band (CB) have shown continuous emission at RT.[3] However, the achievement of a QC laser emitting at short wavelengths at RT appears today still quite challenging in the conventional AlInAs/GaInAs materials due to limited CB offset existing in this material system.[4] Finally, commercial applications of such lasers may be restricted by the use of GaSb substrates and the complexity of the QC laser growth.[5,6]

On InP substrates, the technologically mature InGaAsP QWs system is limited to a 2 μm optical wavelength.[7] This spectral barrier can be broken down by the incorporation of Sb, which leads to a large decrease in the gap. Quantum dot (QD) formation allows one to accommodate large mismatches without dislocation formation. Moreover, a large choice of barrier materials will help to reduce the inter-valence-band absorption. QD lasers are also expected to operate efficiently at higher temperature because of the low Auger recombination induced by the zero-dimensional density of states, and the lower carrier concentration at threshold. Consequently, in order to extend the wavelength emission on InP substrates beyond 2 μm, we propose to use InAsSb QDs. Laser emission from InAsSb QDs grown on InP have been recently reported at 1.96 μm.[8] In this article, we show that longer wavelength emission is achievable in this materials system. We discuss the effect of strain on InAsSb band gap and on the band lineup for various compositions of the barrier (InP, GaInAsP, GaAsSb). We study also Auger recombination and intersubband absorption, which can be important in the choice of the optimum structures.

We have used a simplified theoretical model that takes into account strains, band lineups, and anisotropic and inhomogeneous effective masses.[9,10] With such a model, comparison between various alloys in the QD or in the barrier may be easily performed. The strained 8×8 $\mathbf{k}\cdot\mathbf{p}$ Hamiltonian for the bulk strained InAsSb alloy in the QD is used to calculate the dispersion curves and effective masses for the alloy strained on InP substrate at $T=0$ K. In the strained and flat QD, we make the hypothesis of a constant strain in the QD and a negligible heavy hole (HH)-light hole band mixing.[11] A one-band Hamiltonian and an envelope approximation are then used both for the conduction and valence (HH) bands to calculate the energy levels and the wave functions inside the QD. An excitonic correction calculated by a first-order perturbation expansion is added for the optical interband transition energy. Finally, the transition energy may be shifted as a function of temperature according to the band gap dependence of bulk materials. The material parameters were taken mainly from two references,[12,13] and values for conduction-band energies, valence-band (VB) energies, and gaps are reported in Table I for studied materials.

Figure 1 shows the variation of the band lineups at $T=300$ K as a function of Sb concentration in a bulk strained $InAs_{(1-x)}Sb_x$ alloy grown on an InP substrate. The energy values are given relative to the InP VB energy, which is arbitrarily set equal to zero. The variation of $InAs_{(1-x)}Sb_x$ CB and HH band edge energies are represented by straight lines. VB and CB band edge energies for InP and InGaAsSb barrier materials are represented by dashed and dotted lines, respectively. Other barrier materials are also considered, and values for conduction-band and valence-band energies are reported in Table I for better comprehension. The first obser-

[a]Electronic mail: charles.cornet@ens.insa-rennes.fr

TABLE I. Band lineups at $T=300$ K used in the calculations for several barrier materials and Sb-based strained heterostructures. $Q_{1.18}$ is the $In_{0.8}Ga_{0.2}As_{0.435}P_{0.565}$ quaternary alloy. E_{HH} is the heavy hole valence-band energy. E_{CB} is the electronic conduction-band energy. E_G is the gap energy. Reference is taken as zero for the valence-band energy E_{HH} of InP.

Parameters in eV	InP	$Q_{1.18}$	$GaAs_{0.5}Sb_{0.5}$	$In_{0.52}Al_{0.29}Ga_{0.19}As$	InAs	$InAs_{0.5}Sb_{0.5}$	InSb
E_{HH}	0	0.190	0.892	0.225	0.549	1.087	1.566
E_{CB}	1.35	1.231	1.619	1.354	0.959	1.315	1.890
E_G	1.35	1.041	0.727	1.129	0.410	0.228	0.324

vation is that the minimum of the bulk strained $InAs_{(1-x)}Sb_x$ band gap value (0.22 eV for xSb$\sim$0.5 at $T=300$ K) is larger than for the bulk unstrained alloy. The emission wavelength for such a material is then limited at RT to a maximum of about 5 μm. We may also deduce that the $InAs_{(1-x)}Sb_x$/InP lineup is of type I for xSb<0.5, of type II for $0.5<x$Sb<0.8 and of type III for $0.8<x$Sb<1.0. These results are in good agreement with previous calculations on pure InAs or InSb.[14,15]

Three other materials were considered in the barrier. $In_{0.8}Ga_{0.2}As_{0.435}P_{0.565}$ ($Q_{1.18}$) and $In_{0.52}Al_{0.29}Ga_{0.19}As$ alloys are two examples of lattice-matched quaternary materials used in the active region as optical confinement layer in InP-based lasers emitting at 1.55 μm. $Q_{1.18}$ material has a gap emission wavelength at about 1.18 μm. Following values from Table I, higher CB discontinuity and a longer type I lineup may be expected for the $InAs_{(1-x)}Sb_x$/InAlGaAs system. Finally, we also added in Fig. 1 band lineups for the $GaAs_{0.5}Sb_{0.5}$ alloy lattice-matched to InP (named GaAsSb on Fig. 1), which might be interesting for two reasons: first, it adds a strong confinement in the CB and second, the $InAs_{0.5}Sb_{0.5}$/$GaAs_{0.5}Sb_{0.5}$ growth may be obtained by only switching the gallium/indium beams that leads to a better interface quality. Moreover, this system is analogous to the well-known InAs/GaAs system, which presents a large lattice mismatch ($\sim$7%). The inclusion of the same amount of Sb atoms both in the QD and in the barrier shifts the band gap energies to smaller values.

Figure 2 is an illustration of the strain-induced effects on carriers effective masses. Evolution of the electron mass as a function of Sb composition in unstrained $InAs_{(1-x)}Sb_x$ alloys is compared to the same variation for in-plane (m_r) and out-of-plane (m_z) masses in strained $InAs_{(1-x)}Sb_x$ alloys. We may notice that effective masses are larger in the strained case than in the unstrained case. Therefore, anisotropy induced by strains cannot be neglected.

An increase of the optical interband band gap energy is usually associated with quantum confinement of carriers in QD. As considered above, the emission wavelength for $InAs_{(1-x)}Sb_x$ alloys is limited by strain effects at RT to a maximum of about 5 μm. This upper limit may be further reduced by the additional effect of quantum confinement in the QD. In order to simulate this effect, we have considered a typical QD nanostructure (Fig. 3) with height and diameter equal, respectively, to 5 and 35 nm, embedded into the four material barriers (Fig. 1 and Table I). Inset shows band lineups of the $InAs_{0.5}Sb_{0.5}$/$GaAs_{0.5}Sb_{0.5}$/InP system at 300 K, drawn from values of Table I. It presents clearly that type I band lineups can be obtained for Sb composition close to 0.5 with the $GaAs_{0.5}Sb_{0.5}$ barrier material. Figure 3 shows the QD fundamental transition energy for each barrier material versus the Sb concentration of InAsSb QD limited to the case of a type I band lineup. For $In_{0.8}Ga_{0.2}As_{0.435}P_{0.565}$, InP, and $In_{0.52}Al_{0.29}Ga_{0.19}As$, the Sb concentration is limited to xSb=0.45, 0.47, and 0.53, respectively. In the case of the $GaAs_{0.5}Sb_{0.5}$ material, it is somewhat different because the xSbconcentration is in the [0.37–0.74] range. We notice,

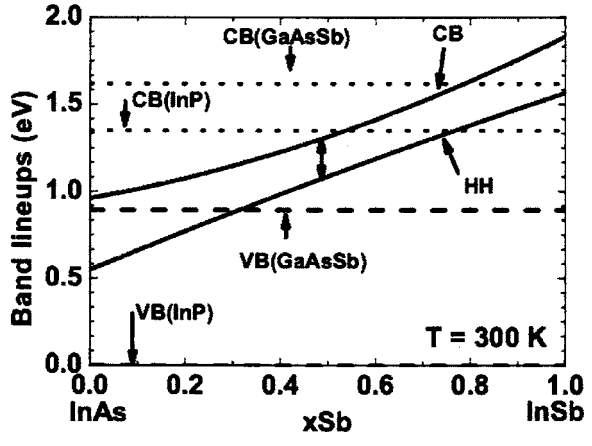

FIG. 1. Variation of the band lineups at $T=300$ K as a function of Sb concentration in a bulk strained $InAs_{(1-x)}Sb_x$ alloy grown on an InP substrate, relative to the InP VB. The variation of $InAs_{(1-x)}Sb_x$ CB and HH band edge energies are represented by straight lines. VB and CB edge energies for InP and GaAsSb are also represented.

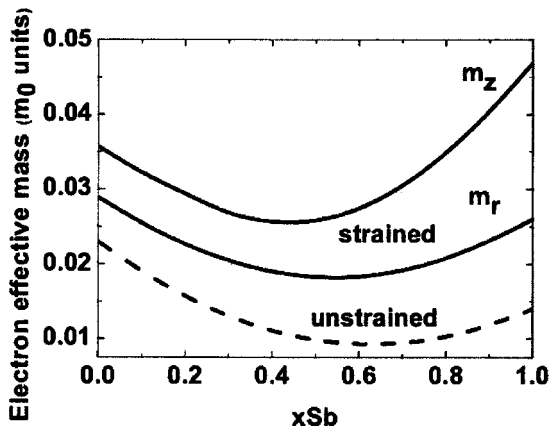

FIG. 2. Evolution of the electron effective mass in free electron mass (m_0) unit as a function of Sb composition in unstrained $InAs_{(1-x)}Sb_x$ alloys compared to the same variation for in-plane (m_r) and out-of-plane (m_z) masses in strained $InAs_{(1-x)}Sb_x$ alloys.

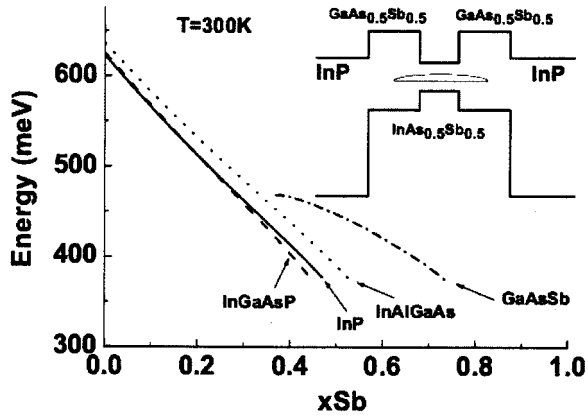

FIG. 3. Variation of the QD fundamental transition energy at $T=300$ K for each barrier material versus the Sb concentration of InAsSb QD for structures presenting only a type I band lineup. The barrier materials considered are $In_{0.8}Ga_{0.2}As_{0.435}P_{0.565}$, InP, $In_{0.52}Al_{0.29}Ga_{0.19}As$, and $GaAs_{0.5}Sb_{0.5}$. Inset shows band lineups of the $InAs_{0.5}Sb_{0.5}/GaAs_{0.5}Sb_{0.5}$/InP system.

however, that in all the four cases, the maximum of the emission wavelength in type I band-lineup regime is shifted from 5 μm to around 3.3 μm (optical transition energy equal to 370 meV) for the examined dot dimensions of 5 nm height and 35 nm diameter. This shift appears due mainly to quantum confinement effect in addition to strain effect. To reach a wavelength above 3.3 μm, larger dot dimensions or quantum dash structures are required in order to decrease the confinement energy.

Some other aspects are important for the realization of laser working at RT. Figure 4 shows the evolution of the spin-orbit split-off (SO) energy as a function of arsenic concentration yAs in the quaternary alloys $In_{1-x}Ga_xAs_yP_{1-y}$ lattice matched to InP at $T=300$ K. It appears that the SO energy falls in the range of the 3.5 μm (0.35 eV) optical wavelength for the $In_{0.53}Ga_{0.47}As$ ternary alloy. Intra-VB transitions in the barrier may then induce large optical losses and thus reduce the efficiency of the main QD optical transition. In order to avoid these losses, barrier materials with large differences between SO energies and emission energies are required. For this reason, it might be advisable to consider $InAs_{(1-x)}Sb_x/In_{0.8}Ga_{0.2}As_{0.435}P_{0.565}$/InP growth

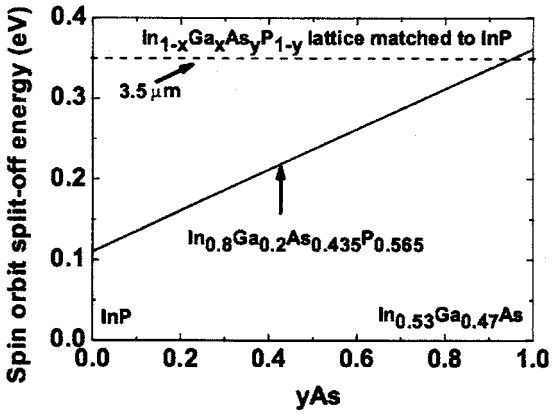

FIG. 4. Evolution of the spin-orbit SO energy at $T=300$ K as a function of arsenic concentration yAs in the quaternary alloys $In_{1-x}Ga_xAs_yP_{1-y}$ lattice matched to InP compared to the energy corresponding to 3.5 μm optical wavelength.

with low SO energies in the barrier for $In_{0.8}Ga_{0.2}As_{0.435}P_{0.565}$ (0.21 eV) and InP (0.11 eV). In the case of the $GaAs_{0.5}Sb_{0.5}$ material, the value of the bowing for the SO parameter is somewhat uncertain.[12] If a bowing parameter equal to 0.6 eV is assumed, the SO energy for the barrier material is found equal to 0.4 eV. Such a low value may affect the performances of devices with $InAs_{(1-x)}Sb_x/GaAs_{0.5}Sb_{0.5}$ in the active region. In the case of InAlGaAs alloys lattice matched to InP, the situation may also be less favorable since the SO energy is always close to the value of 0.35 eV ($\sim$3.5 μm), whatever the alloy composition.

In conclusion, we have studied theoretically the possibilities offered by the growth of InAsSb QD on InP substrate for the realization of midwave infrared emitters. Various materials within the barrier have been considered. Among them, the $InAs_{0.5}Sb_{0.5}/GaAs_{0.5}Sb_{0.5}$ QD may provide a low-energy emission with a system similar to the well-known InAs/GaAs system. Strain and quantum confinement effects may limit the extension towards high emission wavelengths of these nanostructures. By simulating a QD with typical dimensions and type I band lineup, we have found a maximum wavelength of about 3.5 μm. Moreover, a resonance between the main optical transition energy and the intra-VB transition energy in the barrier should occur. The use of various material associations such as $InAs_{(1-x)}Sb_x/In_{0.8}Ga_{0.2}As_{0.435}P_{0.565}$/InP offer possible solutions to limit these problems. However, the growth of large size QDs or quantum dashes, with partial relaxation of strain within the QD, should favor the emission at wavelengths beyond 3.5 μm. By considering a Type II band lineup in further investigations, despite a reduced overlap between electron and hole wave functions, smaller optical transition energies are expected.

[1] J. G. Kim, L. Shterengas, R. U. Martinelli, and G. L. Belenky, Appl. Phys. Lett. **83**, 1926 (2003).
[2] P. Adamiec, A. Salhi, R. Bohdan, A. Bercha, F. Dybala, W. Trzeciakowski, Y. Rouillard, and A. Joullié, Appl. Phys. Lett. **85**, 4292 (2004).
[3] J. Faist, F. Carpasso, D. L. Sivco, C. Sirtori, A. L. Hutchinson, and A. Y. Cho, Science **264**, 553 (1994).
[4] J. Faist, F. Carpasso, D. L. Sivco, A. L. Hutchinson, S. N. G. Chu, and A. Y. Cho, Appl. Phys. Lett. **72**, 680 (1998).
[5] C. Zhu, Y. G. Zhang, A. Z. Li, and Y. L. Zheng, Semicond. Sci. Technol. **20**, 563 (2005).
[6] C. T. Foxon, J. Cryst. Growth **251**, 1 (2003).
[7] M. Oishi, M. Yamamoto, and K. Kasaya, IEEE Photonics Technol. Lett. **9**, 431 (1997).
[8] Y. Qiu, D. Uhl, and S. Keo, Appl. Phys. Lett. **84**, 263 (2004).
[9] P. Miska, C. Paranthoen, J. Even, O. Dehaese, H. Folliot, N. Bertru, S. Loualiche, M. Senes, and X. Marie, Semicond. Sci. Technol. **17**, L63 (2002).
[10] P. Miska, J. Even, C. Paranthoen, O. Dehaese, A. Jibeli, M. Senes, and X. Marie, Appl. Phys. Lett. **86**, 1 (2005).
[11] M. A. Cusack, P. R. Briddon, and M. Jaros, Phys. Rev. B **56**, 4047 (1997).
[12] I. Wurgaftman, J. R. Meyer, and L. R. Ram Mohan, J. Appl. Phys. **89**, 5815 (2001).
[13] S. L. Chuang, *Physics of Optoelectronic Devices*, in Wiley Series in Pure and Applied Optics (Wiley, New York, 1995).
[14] T. Utzmeier, G. Armelles, P. A. Postigo, and F. Briones, Phys. Rev. B **56**, 3621 (1997).
[15] C. Platz, C. Paranthoën, N. Bertru, C. Labbé, J. Even, O. Dehaese, H. Folliot, A. Le Corre, S. Loualiche, G. Moreau, J. C. Simon, and A. Ramdane, Semicond. Sci. Technol. **20**, 459 (2005).